# VIRTUAL PROVING GROUND FOR NETWORKS OF SEISMIC UNATTENDED GROUND SENSORS

Mark L. Moran*, Stephen A. Ketcham, Thomas S. Anderson

USACE Engineer Research and Development Center
Cold Regions Research and Engineering Laboratory
Mark.L.Moran@ERDC.usace.army.mil

Roy J. Greenfield
Greenfield Associates
State College, PA 16801, roy@geosc.psu.edu

## ABSTRACT

Objective Force commanders will be critically reliant on sophisticated networks of sensors to provide seamless situational awareness and area surveillance across a wide range of terrains and operational conditions including tactically important mountainous and urban environments. Unattended Ground Sensor Systems (UGS) will be "nodes" in the Objective Force's sensor network providing unique non-line-of-sight capabilities over multi-kilometer scale areas. However, the battlefield environment has a 1st order effect on core UGS system functions including vehicle tracking and classification. These environmentally driven performance variations must be compensated for to achieve the requisite level of information continuity and accuracy from UGS networks.

Using massively parallel computational resources (provided through a DoD HPC Challenge Grant) and state-of-the-art numerical methods, we have developed a virtual proving ground for simulating the performance of networks of seismic UGS systems. Relying on simulated data we demonstrate methods that allow a network of intelligent seismic UGS systems to "self adapt" to very complex geologic environments. Hardware comparable to this virtual test is not expected for at least 5 years. Our demonstration indicates we have solved the problem of "unknown" geologic effects on seismic signals and furthermore, that seismic UGS networks offer the potential for achieving robust target tracking performance under very difficult atmospheric and geologic conditions. Lastly, full wavefield simulations with this level of fidelity can be used directly for system specific engineering in the same manner as field data saving millions of dollars in field tests.

## 1. INTRODUCTION

Comprehensive, reliable, situation information is imperative for the success of light-armor, maneuver dominated FCS operations. It is almost axiomatic, that tactically significant terrain includes large-scale physiographic features (such as forests, hills, passes, narrow valleys, or rivers). These complex battlefield environments are extremely difficult sensor settings. We can further expect that sophisticated opposing forces will adapt their counter operations to maximally exploit poor sensor coverage circumstances. In these complex settings/contexts passive seismic and acoustic UGSs will provide unique non-line-of-sight (NLOS) and beyond-line-of-sight (BLOS) information under conditions that are poorly covered by air breathing or spaced based sensor platforms. The NLOS attribute is a result of readily "bending" signal wavefronts as they propagate through geologic and atmospheric media. Unfortunately, the inherent variability of terrain and meteorology also leads to large fluctuations in signal characteristics and consequently severe degradations in information accuracy and reliability. These environmental and terrain induced information degradations can be mitigated by deploying high population sensor networks, by

calibrating each UGS node to its specific setting, and by fusing diverse sensor information with optimized algorithms.

Seismic sensors have, historically, not been heavily relied upon in practical tactical systems. This is largely due to the strong effects of geology on the character of seismic data and the highly variable, unknown geologic characteristics of each deployment setting. Geologic adaptation is the central demonstration of this paper. We also address the more general problem of how target-track data fusion for a large number (greater that 6) of spatially distributed UGS sensors can be done and the consequent improvement of tacking accuracy.

# 2. METHODS

The ability to simulate high-fidelity, time-varying, seismic wavefields that include realistic signal complexity is central to our demonstration of seismic sensor geologic adaptation and to our development of optimized track-location information fusion methods. It is particularly important that the signal complexity include the dynamic harmonic energy shifts characteristic of moving targets, and the effects of strong geologic contrasts (large variations in amplitude, coherence, and wavefront curvature).

## 2.1. FDTD Seismic wave simulation

Seismic waves are simulated using a parallel FDTD method described in Moran et al., 1999, Ketcham et al., 2000, and Hestholm and Ruud 1998. The method incorporates surface topography with an appropriate stress-release surface boundary condition into a FDTD viscoelastic wave propagation model featuring 8th-order, staggered-grid, finite-difference operators. Topography is represented by a curvilinear grid transformation that proportionally stretches the FD grid in the vertical direction to match the topography. It is only through the highly efficient Hestholm and Ruud (1998) transformations that seismic propagation modeling with topography can be done on the scales required to support simulations at practical scales. The model can perform either elastic or viscoelastic analyses allowing representation of large energy losses in soils. Discussion of the viscoelastic formulation can be found in Ketcham et al, 2001. FD calculations support wave propagation within a bounded region. Our seismic model has been extensively validated against other numerical models (Ketcham et. al. 1999). More importantly are the recent one-to-one comparisons with field data from the Smart Weapons Test Range, Yuma Proving Ground (Miller et al., 2001). In these direct comparisons we show excellent synthetic waveform agreement with impulsive source data including amplitude, attenuation rate, dispersion, and spectral decay. In practice, such comprehensive agreement with field data is rarely accomplished and lends extensive credibility to the simulations underlying our network tracking analysis.

## 2.2. Moving tracked vehicle source

We excite seismic waves for a notional tracked vehicle in the FD simulation following the method given in Ketcham et al. (2000). The approach applies a sequence of pressure peaks at each FD node point over the entire path of the vehicle. Each pressure peak corresponds to a road-wheel passage. The applied force history for each forced FD node along the vehicle path is very similar in character to measured pressure histories observed in near-surface soil beneath a slow moving armored tracked vehicle. The duration of each node's total force time-history and the peak-to-peak interval between individual road-wheel pulses is proportional to the vehicle speed.

## 2.3. Geologic Model and scale of the computation

The simulations use a notional geology characteristic of many problem spots in the world. The geology has stiff soil layers (above and below a water table) overlying granitic bedrock. Two common geological features distinguish its gently sloping topography: an outcropping of the bedrock and a ravine representative of an eroded streambed. Figure 2 illustrates these features with a road to be traversed by the notional vehicle. In the present demonstration we used an elastic material representation in the original FD model. The material properties are given in Table 1. Viscoelastic effects are added in a post-processing method that gives an effective Qp of roughly 20, and Qs of roughly 10. This is a common attenuation value in near surface soils. The geology represented in Figure 2, is much more complex than is typical for most proving. Thus, a demonstration of accurate seismic network tracking in this terrain constitutes a severe development test.

The geologic model is 750 m by 750 m in extent by 100 m thick. The FD grid had an even spacing interval of 2.8 m. The speed profile for notional tracked (Figure 1b), vehicle requires roughly 60 seconds to traverse the path shown in Figure 2A. The FD time step interval was roughly 0.00034 s. The total number of time steps needed to simulate 60 s of moving vehicle data was 175,700. The calculations were preformed on CRAY T3E-1200 using 128 processors. Wall-clock time was 60 hours. This is likely to be the largest single FD seismic simulation ever preformed. It also demonstrates that seismic FD calculations can be preformed on a scale useful for practical UGS system network performance.

### 2.4. Network geometry and target location tracking

The grided, time-stepping, nature of the FDTD solution approach allows deployment of virtual ground motion sensors at any place in the simulation space. Figure 3A shows a network of 14 virtual seismic UGS nodes deployed with a mean separation between each node of 120 m. In principle, we could deploy a much higher population of UGS Network. Comparable networks with physical hardware are not expected for a number of years. Each UGS node utilizes an array of 6 vertical ground motion transducers (geophones) arranged in a circular pattern having a 3 m radius. In field trials Moran and Greenfield (1997, 1998), and Greenfield and Moran (1998), have demonstrated that this configuration can provide robust LOB tracking of moving vehicles.

The methods used to estimate a LOB and range to a moving ground vehicle with an single array of seismic sensors, such as that given in Figure 3B, are given by Moran and Greenfield (1997), Greenfield and Moran (1998), and Moran et al. (1998). In summary, the LOB determination uses 2-D frequency-wavenumber domain spectral estimation methods (such as Maximum Likelihood, MUSIC, and Normal beamforming). A LOB track result using these methods on field data is shown in Figure 4A.

The range estimation methods use a simple "radar-equation" model with geometric and exponential decay terms. The approach is discussed in Moran et al. (1998a). An example of a range track from this study is given in Figure 4B. The simplistic range estimation model is particularly reliable in the case of seismic surface waves since the dominant term in the expression is the exponential decay (see Ketcham et al., 2001). Furthermore, the vast majority of the seismic signal energy propagating at extended ranges are in seismic surface waves (generally the fundamental Rayleigh mode). This is long wavelength 2-D propagation confined to the surface of the earth-air interface. An individual node can give target position directly from both Range and LOB information. A network is formed when individual UGS nodes exchange target LOB and range information to form a more accurate target track than an independently operating node.

In the present work we apply a Chi-Square data fusion method described in Greenfield and Moran (2001, equation 1). This is an optimal, non-linear, weighted least-squares, error minimization approach. We call this the WLS tracking method. We also estimate the target track using an outlier rejection approach based on the information standard deviations relative to the mean estimated target location. For convenience we label this OLR method. An example of the outlier rejection is shown Figure 5. It gives good results when information for a single sensor type is used.

Geology can be highly variable across geographic regions and within a specific location. These variations have first order effects on the character of seismic signals and must be compensated for before seismic sensors can be employed in battlefield systems. For basic seismic system operation, only two geologic parameters are required. These include the propagation speed of the incoming seismic surface waves, and the rate of decay of surface waves. Using simulated data we show that these basic properties are easily derived from simple calibration methods. We further demonstrate that target tracking information can be corrected allowing compensation for very complex signal effects resulting from strong geologic contrasts. We then demonstrate that target tracks to moving vehicles are substantively improved by application of the correction functions and geology parameters derived from the calibration events.

## 3. RESULTS

Geology can be highly variable across geographic regions and within a specific location. These variations have first order effects on the character of seismic signals and must be compensated for before seismic sensors can be employed in battlefield

systems. For basic seismic system operation, only two geologic parameters are required. These include the propagation speed of the incoming seismic surface waves, and the rate of decay of s.urface waves. Using simulated data we show that these basic properties are easily derived from simple calibration methods. We further demonstrate that target tracking information can be corrected allowing compensation for very complex signal effects resulting from strong geologic contrasts and that incorporating these adaptations lead to substantively improved target tracking.

### 3.1. Calibration Simulation and adapted network locations

Using the geology shown in Figure 2 and our 3D seismic propagation code, we generated a time sequence of the evolving seismic wavefield for a sequence of eight vertical impulse forces applied to the earth's surface along the expected path of the vehicle. The impulses are initiated at 1 s intervals, giving the wavefields time to propagate across the entire model domain. Figure 5 shows the vertical ground motion generated from the 3rd calibration impulse. The locations of the other impulses are indicated with "stars." The positions of each UGS node in the network are also shown. The entire animation spans 8 seconds. Over the course of the entire 8 second wavefield animation we observe over 30 dB of signal amplitude variation, 60 degrees surface wave ray deflection, and dramatic reverberations and reflections from the contrasting geologic features.

Given the network geometry we can extract seismic sensor array data from the simulation result for each of the 14 network nodes. These time series data are processed identically to field data allowing LOB and range estimates to each impulse. Given the known location of each impulse we readily derive estimates of the Rayleigh wave propagation velocity and the attenuation exponent needed for range and LOB estimation.

With the basic geology parameters in-hand, we can also compare the estimated event location to the true event location for each pulse. Representations of these comparisons are shown in Figure 6. As seen in the animated wavefields, the geologic materials between the calibration source and the sensor can severely distort the amplitude and direction of the incoming wavefield. This leads to significant, but *PREDICTABLE*, differences in the estimated LOB and range estimates. A LOB and range correction function can be formed over the range and LOB observation interval (as shown in figure 6). These correction functions are developed for each node in the network.

Figure 7 shows the network accurately estimates the location of all eight calibration events when the correction functions are applied. Without compensation, the geologically induced signal variations causes severe errors in both the LOB and range estimates, leading to poor event locations. In effect, the correction functions allow each UGS node to adapt to its each specific geologic setting. The mean error of the adapted network locations is 42 m, with a standard deviation of 54 m. The error for calibration events within the main body of the network drops to less than 15 m. Calibration event number 5 has a position error of only 2 m. The uncorrected network locations ("raw") have a mean error of 97 m with a standard deviation of 54 m. It is important to stress that the adaptation will improve with greater calibration coverage. In fact, we would expect the largest adaptation benefit from a source that is applied continuously over the likely vehicle path. The vehicle used to deploy the array would be likely to provide the needed seismic excitation energy.

### 3.2. Moving vehicle simulation and adapted network location track

In this section we demonstrate that the geologic tracking parameters and the LOB and range correction functions, derived from the calibration events, can be applied to the problem of tracking a moving vehicle. Figure 8 shows time series for the center element in each UGS node's seismic array and a spectrogram for node 4's time series. The time series shows complex signal behavior with amplitudes that decay rapidly with increasing source distance from the sensor. The spectrogram for node 4, shows appropriate non-stationary spectral energy shifts in proportion to the speed of the vehicle (see Figure 1).

In Figure 9 we give an overlay of the true target LOB and Range with the estimated adapted and raw LOB and range estimates from each UGS node in the network. In the vast majority of the cases the geologically adapted LOB and range estimates show much better correspondence to the true target position. Using only the adapted sensor network range and LOB information, Figure 10 shows the

fused network tracking result using the WLS approach and the OLR approach. The plot shows the true target position at 0.5 s intervals. To give a sense of the shape of the tracking error we use a thin line to connect the WLS and OLR target location estimates the true location. The figure shows that both methods provide an acceptable tracking result. At early times in the vehicle drive through, the error is fairly large. This is a result of poor sensor coverage and the very complex wavefield interactions with geology. The tracking error drops significantly as the vehicle leaves the vicinity of the rock-outcrop, crosses the ravine and enters the main body of the network. The minimum track error (approximately 2 m) is achieved just as the vehicle leaves the ravine. We expect that the WLS method will improve tracking error more rapidly then the OLR method as the number of sensors increase and when additional sensor data is fused.

Figure 11 compares the OLR track using the adapted network to OLR method using the unadapted network track information. This presentation emphasizes the geometric and geologic controls on the character of tracking error. In gross summary, the adapted network has a mean track error of 50 m with a STD of 37 m. The error reduces to roughly 2 m as the target exits the ravine and enters the main body of the network. The unadapted network track has mean error of 113 m with a STD of 80 m. It is interesting to note that the character of the vehicle tracking error closely follows the errors observed in the location of the calibration events. This emphasizes the source invariance and deterministic effects of geology on seismic wave propagation. It also implies that the performance of the network may be fully determined at the time of network deployment.

## 4. CONCLUSIONS

The methods and results presented are founded on state-of-the-art seismic simulations. By using DoD High Performance Computing (HPC) resources we have demonstrated simulations that span kilometer scale spaces and are over 60 seconds in duration. These are critical thresholds for FDTD based simulation support for systems development. The simulation validations against other numerical methods (Ketcham et al, 1999) and direct comparison of waveforms against field data (Miller et al., 2001) lend extraordinary confidence in the accuracy of the simulations results.

The geology used in the simulations has strong heterogeneities that include an out-cropping rock hill and a deep ravine that cuts through a sequence of soil layers. Though this geology is not modeled directly from a specific site it is representative of features encountered in a wide range of geographic locations. The signal complexity that the geology generates is much more severe than those generally encountered at DoD proving grounds.

We fuse LOB and Range information from each node in the network with two methods. The simplest is an outlier rejection (OLR) method based on the mean and standard deviation of each individual nodes location estimate. The second approach uses an optimum non-linear, weighted, least-squares error minimization (WLS) with weights determined from the information (Lob and range) variance. Both these approaches are shown to give comparable performance. However, we expect the WLS approach to be more appropriate with higher network node populations and when considering more diverse sensor inputs.

Using a sparse sequence of calibration events we demonstrate that a seismic UGSs network can be adapted to its specific geologic context. All that is required in the suggested calibration method are a consistent source excitation mechanism and meter scale source position accuracy. These simple criteria can be easily met in a wide variety of ways, including monitoring the seismic signals generated by the network deployment vehicle. The geologic adaptation functions, derived from the calibration data, are then applied to the moving target LOB and range estimates for each UGS node in the network. The results show that the adapted and fused moving vehicle network track results smoothly converge to errors as small as 2 m. The surprising correlation between the location calibration errors and the vehicle tracking error indicate that the network performance might be quantifiable at the time of deployment. This would have broad practical utility in designating target engagement points and weapons systems.

## 5. REFERENCES


Cerjan, C., Kosloff, R., and Reshef, M., 1985, A Nonreflecting Boundary Condition for Discrete Acoustic-Wave and Elastic-Wave Equations, Geophysics, V. 50, pp. 705–708.

Greenfield, R.J., M.L. Moran. 1998. Accuracy of seismic and acoustic bearing estimation. Proceedings of IRIS Specialty Group on Acoustic and Seismic Sensing. Johns Hopkins University, MD. Vol. 2, pp. 175-180.

Greenfield and Moran 2001, Monte Carlo Simulation of Seismic Location Errors for Moving Vehicles, Proceedings of MSS Specialty Group on Acoustic, Seismic and Magnetic Sensing. Johns Hopkins University, MD. Oct. 2001.

Hestholm S., and Ruud, B., 1998, 3-D Finite-Difference Elastic Wave Modeling Including Surface Topography, Geophysics, V. 63, pp. 613–622.

Ketcham, S.A., M.L. Moran, R.J. Greenfield, 2000, FDTD Seismic Simulation of Moving Tracked Vehicle, Military Sensing Symposium (formally IRIS), Battlefield Acoustic and Seismic Sensing, Johns Hopkins University, Columbia MD.

Ketcham, S.A, Greenfield R.J., Moran M.L., Anderson, T.A., Hestholm S., 2001, Soil attenuation in seismic simulations; implications for vehicle tracking, Proceedings of MSS Specialty Group on Acoustic, Seismic and Magnetic Sensing. Johns Hopkins University, MD. Oct. 2001.

Miller, R.D., Anderson, T.A., Davis, J.C., Steeples, D., Moran, M.L., 2001, 3-D Characterization of Seismic Properties at the Smart Weapons Test Range, YPG, AZ, Proceedings of MSS Specialty Group on Acoustic, Seismic and Magnetic Sensing. Johns Hopkins University, MD. Oct. 2001.

Moran, M., and Greenfield, R., 1997, Seismic Detection of Military Operations, 97-CEP-511-1, U.S. Army Maneuver Support Battle Laboratory, Ft. Leonard Wood, MO.

Moran, M., Boulanger, P., Greenfield, R., Gilligan, T., 1998a, Range Estimation with Seismic Sensors for Early Detection, Final report 98-CEP-0505, Maneuver Support Battle Lab, U.S. Army Engineer School, Ft. Leonard Wood, MO.

Moran, M., Greenfield, R., Prado, G., Turpening, R., Peck, L., Kadtke, J., Carnes, B., Bass, H., Detsch, R., Hawley, B., and Ketcham, S., 1998b, Seismic Feasibility Study in Support of Hornet, Final report of PM-MCD Seismic Eagle Team, U.S. Army ARDEC, AMSTA-DSA-MCD, Picatinny Arsenal, NJ.

Moran, M., Ketcham, S., and Greenfield, R., 1999, Three Dimensional Finite-Difference Seismic Signal Propagation, Proceedings of the 1999 Meeting of the MSS Specialty Group on Battlefield Acoustic and Seismic Sensing, Report 440000-147-X, ERIM International, Inc., Ann Arbor, MI, pp. 1-12.

Moran, M.L., D.G. Albert. 1996. Source Location and Tracking Capability of a Small Seismic Array. US Army CRREL Report CR 96-8.

Moran, M.L, S.A. Ketcham, R.J. Greenfield. 1999. Three Dimensional Finite-Difference Seismic Signal Propagation. Proceedings of IRIS Specialty Group on Acoustic and Seismic Sensing. Johns Hopkins University, MD.

Moran, M.L., P.M. Boulanger, P.M., R.J. Greenfield. 1998. Seismic Signal Analysis from moving tracked vehicles, Proceedings of IRIS Specialty Group on Acoustic and Seismic Sensing. Johns Hopkins University, MD. Vol. 1, pp. 297-300.

Moran, M.L., D.G. Albert, R.J. Greenfield. 1996. Ground Vehicle Tracking Using a small Seismic Array. Proceeding of the 20th Army Science Conference, Norfolk VA.


## 6. ACKNOWLEDGMENTS


This work was supported by the US Army Office of the Program Manager for Mines, Countermines, and Demolitions in support of Hornet, Raptor, and Rattler-Track3 under MIPR1FPIC00544 and MIPR1APIC0051. Additional funding was given by the US Army Corps of Engineers, Engineering Research and Development Center, Cold Regions Research and Engineering Laboratory (ERDC-CRREL) under PE62784/AT42. Work at Pennsylvania State University was supported by contract DACA89-99-C-0001.

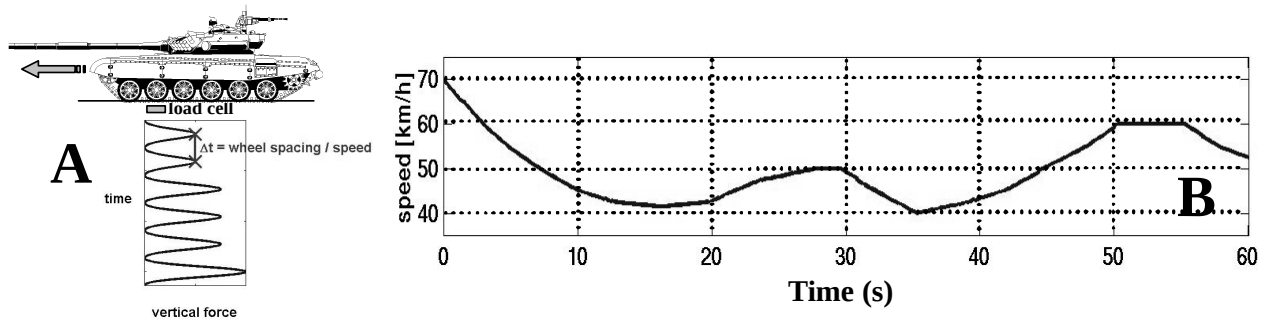


Figure 1. A) Idealization of force vs. time record from a six-axle tracked vehicle. Each peak in the vertical force history corresponds to a road wheel passage. The interval (Δt) and total time duration of the pulse sequence are proportional to the vehicle speed. B) Vehicle speed profile used in present vehicle simulation

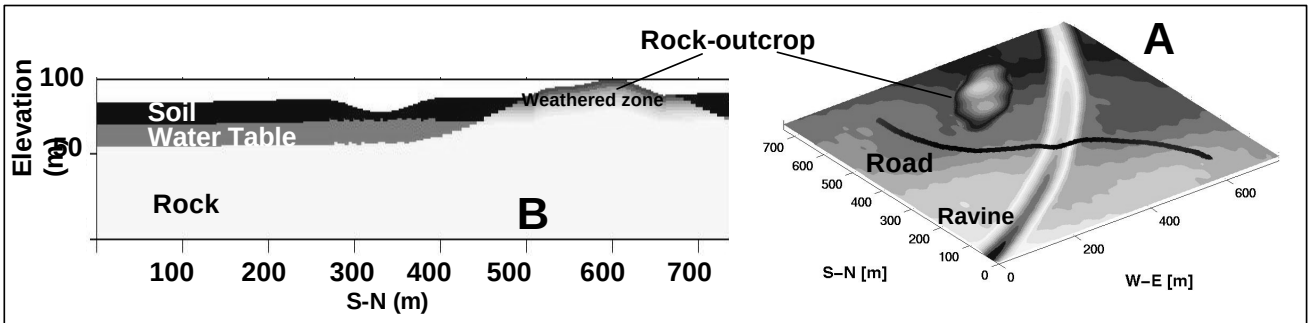


Figure 2. Notional terrain used in seismic simulation. A) Gives the plan view showing road, a ravine and 20 m hill. B) Geologic cross section (west = 375 m) showing the subsurface geology. The ravine and rock-outcrop terminate a stratified soils.

**Table 1. Seismic properties of layer materials in geologic model.**

| **Layer** | **Compression-wave velocity, $V_p$, (m/s)** | **Shear-wave velocity, $V_s$, (m/s)** | **Density, ?, (kg/m$^3$)** |
|---|---|---|---|
| Upper soil layer | 1000 | 577 | 1750 |
| Lower soil layer | 1600 | 625 | 2000 |
| Granitic bedrock layer | 3500 | 2333 | 2650 |

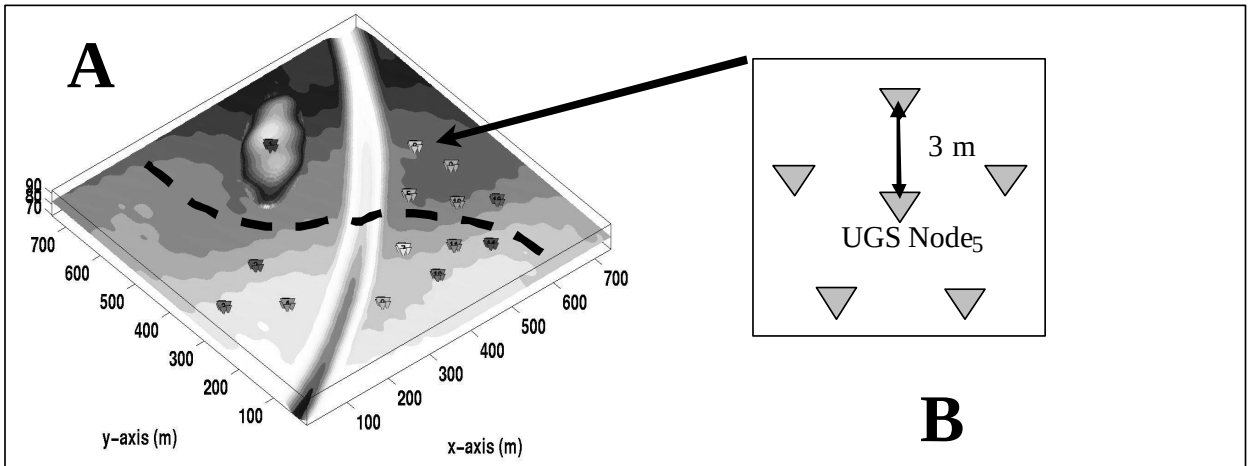


Figure 3. A) Network with 14 UGS seismic nodes. The mean UGS node spacing is roughly 120 m. Future work will optimize and geometry for specific geologic conditions with constraints on node population. B) Enlarged view of UGS node 5 showing arrangement of 6 vertical seismic sensors.

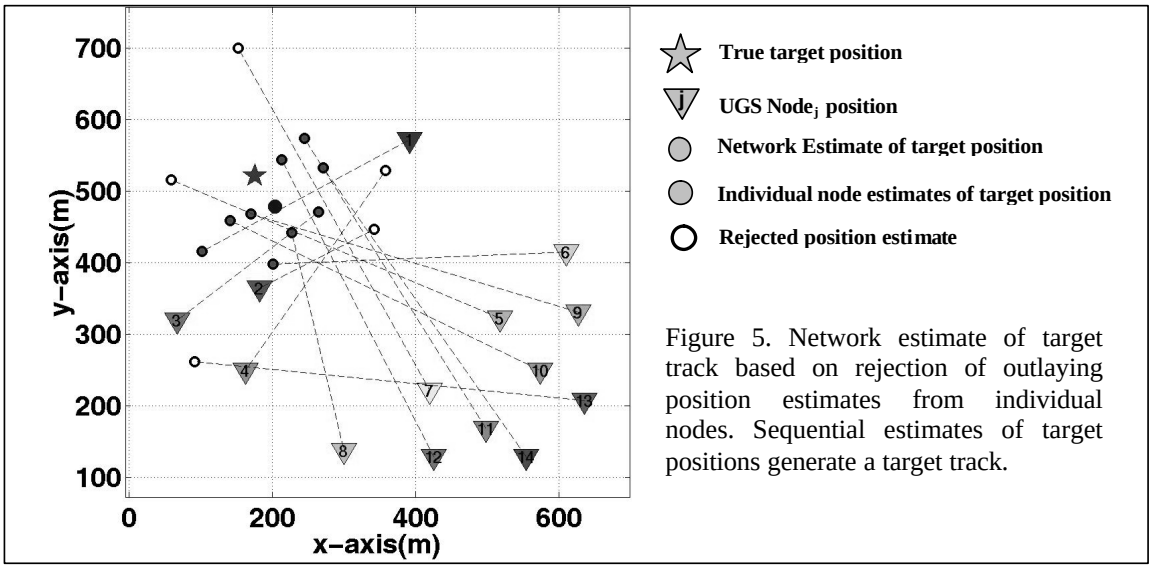


Figure 5. Network estimate of target track based on rejection of outlaying position estimates from individual nodes. Sequential estimates of target positions generate a target track.

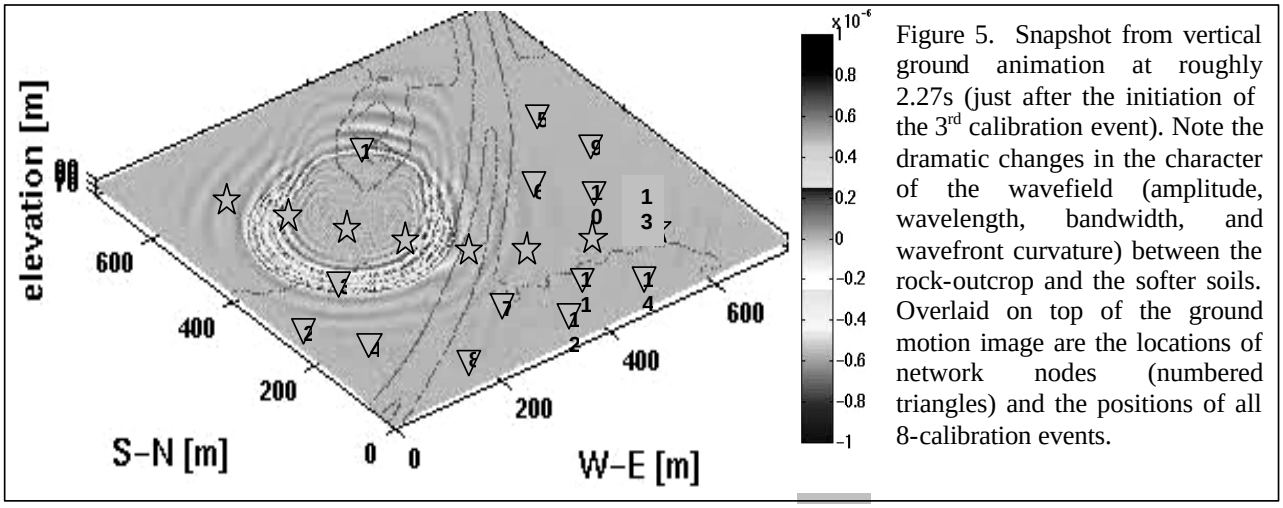


Figure 5. Snapshot from vertical ground animation at roughly 2.27s (just after the initiation of the 3rd calibration event). Note the dramatic changes in the character of the wavefield (amplitude, wavelength, bandwidth, and wavefront curvature) between the rock-outcrop and the softer soils. Overlaid on top of the ground motion image are the locations of network nodes (numbered triangles) and the positions of all 8-calibration events.

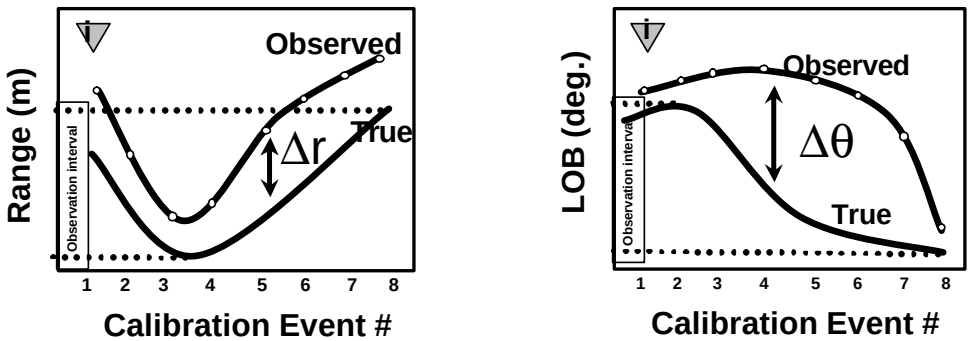


Figure 6. A comparison between the estimated range and LOB and the true LOB and range of each calibration event allows definition of a range and LOB correction function (Δr and Δθ) for each UGS node in the network. When applying these correction functions to moving source data they are only valid within the "observed fit interval" (between dotted lines) A) Estimated Range compared to true range. B) Estimated LOB compared to true LOB.